Expert Opinion on Drug Metabolism & Toxicology

ISSN: (Print) (Online) Journal homepage: https://www.tandfonline.com/loi/iemt20

The safety and toxicity profile of SPL84, an inhaled antisense oligonucleotide for treatment of cystic fibrosis patients with the 3849 +10kb C->T mutation, supports a Phase 1/2 clinical study

Lital Friedman, Ofra-Barchad Avitzur, Efrat Ozeri Galai, Nicolay Ferrari, Asa Choen, Sara Dahan, Tamar Mordechai & Gili Hart

To cite this article: Lital Friedman, Ofra-Barchad Avitzur, Efrat Ozeri Galai, Nicolay Ferrari, Asa Choen, Sara Dahan, Tamar Mordechai & Gili Hart (06 Oct 2023): The safety and toxicity profile of SPL84, an inhaled antisense oligonucleotide for treatment of cystic fibrosis patients with the 3849 +10kb C->T mutation, supports a Phase 1/2 clinical study, Expert Opinion on Drug Metabolism & Toxicology, DOI: 10.1080/17425255.2023.2266361

To link to this article: https://doi.org/10.1080/17425255.2023.2266361

EXPERT OPINION ON DRUG METABOLISM & TOXICOLOGY
https://doi.org/10.1080/17425255.2023.2266361

Taylor & Francis
Taylor & Francis Group

ORIGINAL RESEARCH

The safety and toxicity profile of SPL84, an inhaled antisense oligonucleotide for treatment of cystic fibrosis patients with the 3849 +10kb C->T mutation, supports a Phase 1/2 clinical study

Lital Friedman[a*], Ofra-Barchad Avitzur[a*], Efrat Ozeri Galai[a], Nicolay Ferrari[b], Asa Choen[a], Sara Dahan[a], Tamar Mordechai[a] and Gili Hart[a]

[a]SpliSense, BiohouseLabs, Haddasah Ein Kerem, Jerusalem, Israel; [b]OnTargetxR&D Inc, Boucherville, Quebec

ABSTRACT

Introduction: SPL84 is an inhaled antisense oligonucleotide (ASO) in development for the treatment of cystic fibrosis (CF) patients carrying the 3849 + 10kb C->T (3849) mutation. To support the initiation of the first clinical study, a full battery of safety and toxicology studies were performed.

Research design and methods: SPL84 was administered by inhalation to mice and monkeys to determine the no observed adverse effect level (NOAEL) and establish sufficient safety margins for the starting clinical dose.

Results: There were no preclinical safety findings with SPL84; no related clinical signs, nor any effect on body weight, food consumption, or clinical pathology. The microscopic changes in the lungs were regarded as non-adverse and reflected a normal clearance process for inhaled compounds. Systemic exposure in both species was low. The NOAEL for mice and monkeys was the highest administered dose in both species, resulting in safety margins ~ 40X the proposed starting clinical dose.

Conclusion: These successful results supported the initiation of a phase 1/2 clinical study of SPL84 (ongoing), assessing the safety, tolerability, and pharmacokinetics of a single ascending dose in healthy subjects to be followed by assessment of safety, tolerability, pharmacokinetics, and preliminary efficacy of multiple ascending doses in CF patients carrying the 3849 mutation.

ARTICLE HISTORY
Received 13 June 2023
Accepted 15 September 2023

KEYWORDS
Antisense oligonucleotide; cystic fibrosis; inhalation; safety profile; Toxicokinetics; lung

1. Introduction

Over the past 25 years, antisense oligonucleotide (ASO) technology has been developed and validated as a new platform for drug target discovery and development [1–7]. ASOs are small (12–25 nucleotide) synthetic nucleic acid molecules that bind specific sequences within target ribonucleic acid (RNA) molecules. Their function can be exploited to reduce or restore the expression of target mRNA transcripts. Indeed, ASOs can inhibit the translation of toxic gain-of-function proteins via the activation of RNase H. They may also modulate RNA splicing to promote or restore the expression of partially or fully functional proteins in diseases caused by haploinsufficiency or complete loss of protein [8,9]. Chemical modifications of ASOs confer advantageous properties, such as greater potency, and fewer toxicity and tolerability issues [5]. In each chemical class of ASOs, all drugs have similar structures, and physical and chemical properties, including similar lengths, molecular weight, charge, solubility, and stability. These shared physical-chemical attributes result in drugs with similar pharmacokinetics, potencies, adverse events, and tolerability [6,10–13]. The 2′-O-methoxy ethyl (2′-O-MOE) modification has proven to be one of the most beneficial, and therefore, is the most characterized modification. To date there are five approved ASO drugs with this chemistry, Kynamro®, Spinraza®, Tegsedi®, Waylivra®, and Milasen [14,15].

SpliSense has developed an innovative inhaled ASO, SPL84, specifically designed to treat CF patients carrying the 3849 + 10Kb C->T (3849) mutation within the CFTR gene. SPL84 is a 2′-O-MOE 19-mer splice switching ASO with a phosphorothioate backbone. It is targeted to correct a splicing defect caused by the 3849 mutation in the CFTR gene [16], resulting in the production of normal, fully functional CFTR protein [17,18]. SPL84 fully restored CFTR channel activity in patient-derived nasal and bronchial epithelial cells, thereby demonstrating its potent pharmacologic activity [19].

Most of the ASO drugs currently in development use the systemic route of administration, typically via subcutaneous injection or intrathecally. SPL84 is intended to be administered by inhalation, directly to the target organ (i.e. lungs), in order to increase lung exposure with minimal systemic exposure. The pharmacokinetic and toxicity profiles of phosphorothioate ASOs following intravenous and intratracheal administration have been well established in animals [7,20–24] and in humans [25,26]. However, there is a paucity of published

CONTACT Gili Hart gili@splisense.com SpliSense Biohouse Labs, Haddasah Ein Kerem, Jerusalem, Israel
*These authors are contributed equally to this paper.

Supplemental data for this article can be accessed online at https://doi.org/10.1080/17425255.2023.2266361

studies reporting the pharmacokinetics and toxicity of phosphorothioate ASOs following pulmonary delivery [24,27–29]. Here, we report the results from the nonclinical studies performed to support initiation of a Phase 1/2 clinical study of SPL84 for the treatment of CF.

2. Material and methods

2.1. Antisense oligonucleotides

SPL84 was synthesized as a sodium salt by LGC Biosearch Technologies (Petaluma, CA) and provided for each study as a lyophilized material. Saline for injection USP (0.9%) was obtained from a commercial source (Baxter) and used for dilution of the SPL84 or as a vehicle in control groups in animal studies. SPL84 sequence: CUGCAACAGAUGGAAGACU.

2.2. Specificity assay

Human bronchial epithelial (HBE) cells (from non-CF or CF donors) were expanded in PneumaCult™-Ex Plus Medium (AMP medium). After expansion, cells were seeded on porous filters (6.5 mm Transwell® with 0.4 µm Pore Polyester Membrane Insert 0.33 cm^2 Transwell, Corning) in air liquid interface (ALI) culture. After cell differentiation under ALI conditions, SPL84 was added from the apical side (on top of the mucus), as indicated below.

2.2.1. Electrophysiological experiments - Ussing chamber assay

The short-circuit current (Isc) was measured under voltage clamp conditions with an EVC4000 precision V/I Clamp (World Precision Instruments). Culture inserts with differentiated HBE cells were mounted in Ussing chambers (Physiologic Instrument). For all measurements, chloride (Cl^-) concentration gradient across the epithelium was applied by differential composition of basal and apical physiological solutions. Inhibitors and activators were added after stabilization of baseline Isc: sodium (Na^+) channel blocker Amiloride (100 µM) (Sigma Aldrich) to inhibit apical epithelial Na+ channel (ENaC); cAMP agonists forskolin (10 µM) (Sigma Aldrich) and IBMX (100 µM) (Sigma Aldrich) to activate the transepithelial cAMP-dependent current (including Cl^- transport through CFTR channels); CFTR inhibitor CFTRinh172 (10 µM) (Sigma Aldrich) to specifically inhibit CFTR; and ATP (100 µM) (Sigma Aldrich) to challenge the purinergic calcium-dependent Cl^- secretion. CFTR-specific activity was quantified according to the effect of CFTR inhibitor Inh-172, which determines the relative current contribution of the CFTR channels versus other anion transport pathways [30].

2.2.2. RNA purification

Total RNA from HBEs was extracted using the QIA shredder and RNeasy micro-Kit (Qiagen). Complementary DNA (cDNA) synthesis was performed using the High-Capacity cDNA kit (Applied Biosystems). For evaluation of cryptic exon skipping, RT-PCR was employed to amplify the correctly and aberrantly spliced transcripts using primers aligned to exon 22 and 23, using Platinum™ SuperFi™ Green PCR Master Mix (Invitrogen). PCR Primers: F-5′-ATAGCTTGATGCGATCTGTGA -3′ (exon 22) and *R*-5′-ATCCAGTTCTTCCCAAGAGGC-3′ (exon 23).

2.3. Off-target assay

2.3.1. In silico analysis

This study was performed at Monoceros Biosystems LLC (San Diego, CA). To identify potential off-target genes, a similar strategy to the one recommended by the 'Off-Target Subcommittee of the Oligonucleotide Safety Working Group' [31] was employed. The searches included both mature and primary human transcripts (pre-mRNA), including non-coding RNA and mitochondrial RNA that are aligned (including mismatches) with SPL84 that can potentially lead to off-target gene effects. To further profile the extent of potential safety risks from each potential off-target gene, gene expression in the target lung tissues and main organs of SPL84 drug accumulation, i.e. liver and kidney, were evaluated. Finally, searches for evidence of disease associations with full knockdown or partial knockdown of each potential off-target were performed, and a risk assessment for each gene was conducted. An in vitro potency assessment of potential off-target effects was performed if one of the following risk criteria were met: 1) full match of ≥ 15bp alignment and expression in main organs of ASO accumulation (lung, kidney, and liver), 2) association with a non-recessive genetic disorder and/or mouse pathologies and expression in the main organs of ASO accumulation.

2.3.2. In vitro analysis

This study was performed by exposing HBE cells from homozygous patient carrying the 3849 mutation to SPL84 by free uptake (200 nM). In addition, analysis of PCSK9 and SRPRB gene modulation was performed in HepG2 cells, a hepatic cell line, treated with SPL84 by free uptake (5 µM). Specific primers were designed for PCR analysis for the seven potential off-target genes to assess the probability of gene modulation as a result of treatment with SPL84. RNA extraction and cDNA synthesis analysis of exon skipping was performed using RT-PCR, and the results were run on agarose gel.

For each off-target gene tested, the NCBI Refseq database on the UCSC genome browser was searched for the exact location of the potential off-target binding site, and adjacent exons for gene modulation and exon skipping analysis were selected. If the gene included multiple transcripts, a minimal number of primers that would be adequate to analyze all of the relevant transcripts were designed (Supp Table S8). All transcripts being analyzed for off-target exon skipping were amplified by RT-PCR reaction using primers listed in Supp Table 1. PCR reaction was performed using Platinum SuperFi™ Green PCR Master.

2.4. Peripheral blood mononuclear cell (PBMC) cytokine release assay (CRA)

The PBMC CRA was performed at ImmunXperts (Belgium) with fresh or cryopreserved PBMCs, previously isolated from the blood of healthy donors. PBMCs were thawed in serum-free culture medium (CellGenix), counted and resuspended to

Table 1. Summary of the mean aerosol concentration and estimated overall achieved delivered doses for SPL84 in mouse toxicity study.

				Particle Size		Number of Animals					
						Main		Recovery		TK animals	
Target Dose Level of SPL84 (mg/kg/week)	Target Aerosol Concentration (mg/L air)	Mean Achieved Aerosol Concentration (mg/L air)	Total Achieved Inhaled Dose Level of SPL84 (mg/kg/week)	MMAD (µm)	GSD	Males	Females	Males	Females	Males	Females
0	0	0	0	NA	NA	10	10	6	6	4	4
4	0.0706	0.0888	5.49	1.6	2.18	10	10	-	-	20	20
20	0.353	0.4038	24.2	1.6	2.17	10	10	6	6	20	20
48	0.846	0.907	54.4	1.8	2.16	10	10	6	6	20	20

NA: Not applicable; MMAD: Mass Median Aerodynamic Diameter; GSD: Geometric Standard Deviation; TK: Toxicokinetic.

a suitable concentration. The analysis of cytokines produced in the supernatant was performed by a Luminex® 200 using the 'Multiplex HCYTOMAG-60K-10C' kit according to the manufacturer's protocol (Merck/Millipore). All data were analyzed using Luminex® software xPONENT 3.1 and Excel. Statistical analysis was performed with the statistical software JMP Pro v13 (SAS Institute Inc.,Cary, NC, 1989–2019). All data were logarithmically transformed before analysis. A 2-way ANOVA was performed with donor and condition as predictors, separately for cryopreserved and fresh donors.

2.5. Toxicological studies

2.5.1. Animals

The study plans and relevant amendments were reviewed and approved by the Animal Care Committee (ACC) of ITR. ACC acceptance was maintained on file at ITR. All animals used in the study were cared for in accordance with the principles outlined in the current 'Guide to the Care and Use of Experimental Animals' as published by the Canadian Council on Animal Care and the 'Guide for the Care and Use of Laboratory Animals,' a NIH publication.

Male and female CD-1 mice (Charles River Laboratories, Raleigh, NC) were used for the mouse studies; mice were approximately 6–7 weeks of age (23 to 35 g) at the time of study assignment (Day 1). Male and female cynomolgus monkeys (Macaca fascicularis) were obtained from Worldwide Primates Inc, Miami, FL. At assignment to study, animals were young adults with body weights ranging from 2.8 to 4.2 kg for males and 2.3 to 3.2 kg for females. Prior to study start, mice and monkeys were acclimatized to the study equipment and procedures, such as restraint tubes for mice and chairs and exposure face masks for monkeys).

2.5.2. Study design

All studies were performed at ITR Laboratories Canada (Baie d'Urfe, QC) and at Axolabs GmbH (Germany) supervised by OnTargetx R&D Inc. (Quebec, Canada). For the mouse and monkey dose range finding (DRF) studies, mice were allocated among a saline control group and six SPL84-treated groups (as detailed in Supp Table 2 and Supp Table 3). For both species, SPL84 was administered as aerosols using an inhalation exposure system (chamber for mice and face mask for monkeys) once weekly for 4 consecutive weeks.

For the GLP toxicity studies, SPL84 was administered via inhalation once weekly for 8 consecutive weeks (a total of 9 doses) to mice at achieved dose levels of 0 (vehicle control), 5.49, 24.2, and 54.4 mg/kg/week (Table 1), or to monkeys at achieved dose levels of 0 (vehicle control), 6, 10.9, and 20.8 mg/kg/week (Table 2).

2.6. Aerosol generation and analysis

SPL84 for aerosol generation was formulated in 0.9% saline prepared on each day of usage, and aerosol generated using the Sidestream nebulizer. The target dose levels, aerosol concentrations, and achieved dose levels are detailed in Tables 1 and 2, and Supp Table 2 and Supp Table 3, for the mouse and monkey studies, respectively.

The concentration and stability of SPL84 in the generated aerosol over time were measured on each day of aerosol generation by collecting samples on glass fiber filters. The distribution of particle size in the generated aerosols was measured on each day of aerosol generation by collecting samples into a 7-Stage Mercer Cascade Impactor (except for control groups). All sample substrates obtained were transferred to the analytical laboratory of ITR for the determination of aerosol concentration and particle

Table 2. Summary of the mean aerosol concentration and estimated overall achieved delivered doses for SPL84 in monkey toxicity study.

				Particle Size		Number of Animals			
						Main		Recovery	
Target Dose Level of SPL84 (mg/kg/week)	Target Aerosol Concentration (mg/L air)	Mean Achieved Aerosol Concentration (mg/L air)	Total Achieved Inhaled Dose Level of SPL84 (mg/kg/week)	MMAD (µm)	GSD	Males	Females	Males	Females
0	0	0	0	NA	NA	3	3	2	2
6	0.3342	0.3326	6	1.3	2.1	3	3	-	-
12	0.6649	0.6131	10.9	1.6	2.08	3	3	2	2
25	1.3867	1.1683	20.8	1.9	2.13	3	3	2	2

NA: Not applicable; MMAD: Mass Median Aerodynamic Diameter; GSD: Geometric Standard Deviation; TK: Toxicokinetic.

size of the SPL84 aerosols using a validated analytical method. In addition, in order to demonstrate that SPL84 integrity was maintained following nebulization, representative aerosol samples pre- and post-nebulization were collected and analyzed using a qualified denaturing IPRP-UPLC -MS method.

2.7. Estimation of achieved dose levels

The achieved total inhaled dose levels mentioned in this study were estimated using the following formula:

$D_L = E_c$ x RMV x T/BW
D_L = Achieved dose levels (mg/kg)
E_c = Actual SPL84 concentration (by analytical determination) delivered to the animals (mg/L air)
RMV = Respiratory minute volume (L/min) according to the method of Alexander et al. [32] *RMV* (L) = 0.608 × *BW* (kg)$^{0.852}$
T = Time, duration of daily exposure (min)
BW = Mean body weight (kg) during the exposure period.

In the mouse studies, the parameters were: BW = 0.05 kg, *T* = 60 minute. In the monkey studies, the parameters were: BW = 3 kg, *T* = 35 minutes. The achieved doses for each study are detailed in Tables 1 and 2 and Supp Tables S2, S3.

2.8. Clinical observations

Mice and monkeys were observed daily for mortality and clinical observations. Parameters monitored in animals included mortality, clinical observations, body weight, and food consumption. Ophthalmological examinations were performed for all animals in the mouse and monkey toxicity studies once during the pre-treatment period and at the end of the treatment period (Week 8). A standard hematology and chemistry panel was conducted at the beginning and end of study as well as at recovery. In the monkey toxicity study, additional clinical signs were recorded: at each necropsy, urine was collected directly from the bladder for standard urinalysis. ECGs were performed on conscious animals prior to the initiation of treatment and then subsequent to first and last exposure. Complement factors Bb and C5a were measured at pre-treatment and on Days 1 and 57 at 1-hour and 24-hours after the end of exposure.

2.9. Histopathology

Following the last dose in the toxicity studies, mice or monkeys were euthanized and subjected to a necropsy examination on Day 59. The recovery mice or monkeys were observed for 12 weeks following the last dose and then euthanized and subjected to a necropsy examination on Day 141. For both studies, tissues were prepared for microscopic examination by embedding in paraffin wax, sectioning, and staining with hematoxylin and eosin.

2.10. Bioanalytical evaluation

In the mouse toxicity study, a series of 5 blood samples (approximately 0.5 mL each) were collected from 5 cohorts of 2 toxicokinetic mice/sex/group/timepoint each on Days 1 and 57. In the monkey toxicity study, a series of 6 blood samples were collected from each monkey in all study groups on each of Days 1 and 57. Samples were analyzed using a validated anion-exchange high-performance liquid chromatography (AEX-HPLC) method with fluorescence detection, a hybridization-based assay using a complementary probe that is fluorescently labeled for measurement of SPL84 concentration in plasma.

In the mouse toxicity study, at termination of the TK animals assigned to the 1- and 24-hour post-dose blood collection on Days 1 and 57 (2 animals/sex/group/time point), a small piece (approximately 0.5 g) of lungs, kidney, and liver was collected, snap-frozen in liquid nitrogen, and stored deep-frozen (approximately ≤-60°C) before being analyzed using a qualified AEX-HPLC method with fluorescence detection.

2.11. Toxicokinetic analysis

Noncompartmental analysis (NCA) of the plasma concentration of SPL84 on Days 1 and 57 was performed using Phoenix®WinNonlin®. The following toxicokinetic parameters were calculated: $AUC_{0\text{-Tlast}}$ (area under the plasma drug concentration-time curve from the time of dosing to the last quantifiable concentration), $t_{1/2}$ (terminal elimination half-life), C_{max} (the maximum plasma concentration), and T_{max} (time to maximum plasma concentration).

3. Results

3.1. SPL84 specificity

SPL84 was designed to specifically target and bind a motif within the cryptic exon (84 bp) created by the 3849 mutation. It was previously demonstrated that treatment with SPL84 leads to a complete rescue of CFTR function in primary nasal and bronchial epithelial cells from CF patients carrying the 3849 + 10 kb C->T mutation [19]. As most CF patients carrying the 3849 mutation are heterozygote patients, we determined SPL84 specificity to the 3849 mutation by comparing its binding to the wild-type (WT) or other (non-3849) CF mutation allele. Figure 1 shows the effect of SPL84 in human nasal epithelial (HNE) cells from a CF patient homozygous for the F508del mutation, and in HNE cells from a non-CF healthy volunteer. Results showed that SPL84 had no effect on the WT *CFTR* splicing pattern as measured by RT-PCR (Figure 1a). Moreover, SPL84 treatment of HNE cells from non-CF healthy volunteers and F508del cells did not impair CFTR function as measured by the Ussing assay (Figure 1b, c). As a positive control, we confirmed that treatment with SPL84 led to significant modulation of the splicing pattern, reducing the aberrant splicing and increasing the correctly spliced CFTR in HNE cells from a CF 3849 + 10 kb C->T heterozygote patient (Figure 1d).

Altogether, the analysis showed that the effect of SPL84 was specific to *CFTR* alleles carrying the 3849 mutation with no effect on other CF mutations or WT CFTR sequences.

3.2. SPL84 off-target analysis

Another safety concern dependent on Watson-Crick base pairing is hybridization dependent off-target risks. In contrast to the risk for nonspecific, on-target binding described above, off-target risk relates to the oligonucleotide binding to transcripts other than the intended CFTR target. First, we identified candidates for off-target hybridization of SPL84 by in silico screening [31]. Results revealed that there is no primary or mature RNA with full-length homology or with 1 mismatch complementary to SPL84 among the full array of human genes. Multiple transcripts with two and three mismatches were found. Seven genes which met the in silico risk criteria but were still considered low risk for off-target effect (see Materials and Methods) were selected for an in vitro potency assessment of potential off-target effects (Supp Table 4). Importantly, in all but one of the potential off-target genes, the alignment was to a sequence within an intron, significantly reducing the chance for an off-target effect.

As all selected genes are expressed in the lungs, the unintended effect of SPL84 on the putative off-target genes was analyzed in primary HBE cells derived from a 3849 homozygous patient treated with SPL84 or a control ASO. SPL84 did not influence the expression of any of the genes tested (Supp Figure 1a). As a positive control, we confirmed that treatment with SPL84 led to a significant modulation of the splicing pattern, reducing the aberrant splicing and increasing the correctly spliced *CFTR* (Figure 1d). Similarly, SPL84 treatment of HepG2 cells did not results in changes of the expression levels of PCSK9 and SRPRB which are associated with phenotypes in the liver (Supp Figure 1b). Overall, the in-silico and in-vitro analyses suggested that SPL84 has no prominent risk of eliciting unintended off-target effects.

3.3. Immunogenicity screening of SPL84 in a cytokine release assay

Immunostimulation caused by ASOs, in particular those with phosphorothioate backbones, is a complex side effect that depends on several aspects, including chemistry and nucleotide sequence [33–35]. ASOs can activate the innate immune system through binding to pattern-recognition receptors such as the toll-like receptors (TLRs). The potential inflammatory properties of SPL84 were evaluated in a human PBMC (hPBMC) cytokine release assay. SPL84 had no effect on the secretion of 10 different cytokines, except for a small, significant but highly variable increase in the secretion of 3 cytokines, IFN-γ, IL-10, and MIP-1α (Supp Table 5, Supp Figure 2). However, this increase was significantly lower than that observed when hPBMCs were treated with positive controls such as immunostimulatory reagent (LPS) as well as TLR8 or TLR9 activators (ODN2395, ODN2216, and CL075), which were mainly used to confirm assay integrity and suitability, even at concentrations of SPL84 that were 30-fold higher than the concentration of the positive control (Supp Table 5). Overall, these results confirmed that SPL84 has little to no immunostimulatory properties when compared to the negative control (media).

3.4. Toxicity evaluation of SPL84 in mice and monkeys

3.4.1. Aerosol characterization and estimation of achieved dose levels

The aerosol characterization and estimation of dose levels were done before and during each toxicity study with SPL84. The actual aerosol concentrations of SPL84 in the mouse and monkey studies were dose-dependent, and variation among

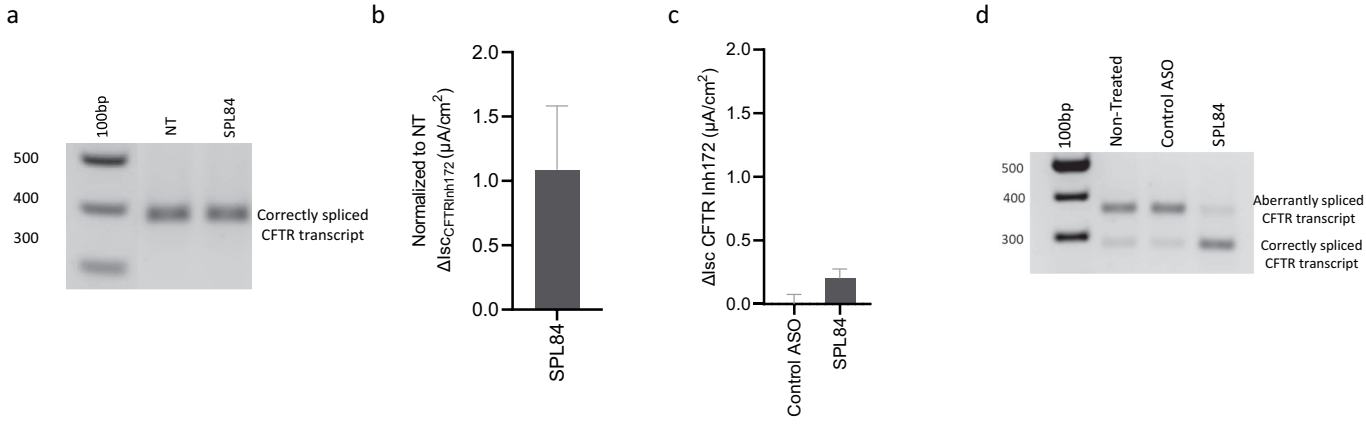

Figure 1. Specificity of SPL84 in HNE cells. A-B. specificity analysis in untreated (NT) or SPL84 treated (200 nM) HNE cells from non-CF healthy volunteers. RNA was extracted and the CFTR splicing pattern of CFTR was analyzed using RT-PCR amplifying a ~ 400bp region between exons 22 and 23 (A). The CFTR activity was measured in the Ussing chamber assay from non-CF HV presented as the median of the absolute ΔIscCFTRInh172 values normalized to NT calculated from 4 filters from one biological experiment (B). C. The CFTR activity was measured in the Ussing chamber assay of HNE cells derived from a homozygous F508del CF patient treated with SPL84 or a control ASO. The effect of the treatments is presented as the median of the absolute ΔIscCFTRInh172 values calculated from 4 filters from one biological experiment. (D) specificity analysis in untreated (NT), control ASO or SPL84 treated (200 nM) HNE cells from CF 3849 + 10 kb C->T heterozygote patient. RNA was extracted, and the CFTR splicing pattern of CFTR was analyzed using RT-PCR amplifying a ~ 400bp region between exons 22 and 23.

the values was low (Tables 1, 2 and Supp Tables 2, 3, respectively). The overall achieved aerosol concentrations for all dose groups were within 20% of the respective targeted SPL84 concentrations. The stability of the aerosol concentration was acceptable since the coefficient of variance (equivalent to the percentage relative standard deviation) of aerosol concentrations between samples was not greater than 20%. No quantifiable levels of ASO were found on the filters collected from the control (saline) groups for each study. The particle size of the nebulized solutions was in the 1.1–1.8 µm and 1.5–2 µm mass median aerodynamic diameter (MMAD) range, which is in the respirable size range for mice and monkeys, respectively. Additionally, the integrity of aerosol samples post-nebulization as compared to pre-nebulization was evaluated, and the results showed that all parameters met the acceptance criteria, indicating that the integrity of SPL84 was maintained following nebulization (Supp Table S6).

3.4.2. 8-week inhalation toxicity study followed by a 12-week recovery period in CD-1 mice and cynomolgus monkeys

The toxicity profile of SPL84 was assessed in mice and monkeys, as these species have been previously recommended by various regulatory authorities as relevant animal models for safety studies. We previously performed 4-week DRF studies in mice and monkeys (Supp Table 2 and Supp Table 3, respectively), using a broad range of doses in order to establish dose levels for the subsequent GLP-compliant studies. In the GLP studies, the toxicity and toxicokinetic profile of SPL84 was assessed following once weekly administration via inhalation for 8 consecutive weeks (for a total of 9 doses) in mice and monkeys (Tables 1 and 2, respectively). The persistence, delayed onset, or reversibility of any changes were assessed during a subsequent 12-week recovery period.

In mice, inhalation administration of SPL84 was well-tolerated with no mortality or adverse clinical signs. There were no effects on clinical signs, body weights, food consumption, clinical pathology parameters (full panels of hematology and clinical chemistry), or organ weights. Microscopic findings associated with SPL84 were noted in the lung, tracheobronchial and mandibular lymph nodes, kidney, and liver (Table 3). Minimal to mild increase in macrophage cellularity with minimal intracellular basophilic granules was noted in the lung (Figure 2) and tracheobronchial lymph node (Figure 3) in mice at doses ≥5.49 mg/kg/week of SPL84 and in the mandibular lymph node and the liver (Kupffer cells) in mice dosed with 54.4 mg/kg/week of SPL84 (Supp Figure 3). Minimal basophilic granulation was observed within the kidney tubules of mice dosed at ≥24.2 mg/kg/week of SPL84 (Supp Figure 4). There was no degenerative change of the alveolar macrophages or other pulmonary cell types and, additionally, there was no inflammatory cell infiltrate present in the lungs. These minimal adaptive changes in the lung, lymph nodes, liver, and kidney were not considered adverse. There were no microscopic findings in any other organs. Following a 12-week recovery period, there was incomplete but progressive ongoing reversal of the microscopic findings in the lung, lymph nodes, and liver and complete reversal of changes in the kidney (Supp Figure S5, Supp Table S7). Given the non-adverse nature of the findings and ongoing recovery, the NOAEL in mice was determined as the highest dose level of 54.4 mg/kg/week.

Table 3. Microscopic changes in the lung, tracheobronchial and mandibular lymph nodes, and kidney and liver – mouse toxicity study.

		Male				Female			
	Dose (mg/kg/week)	0	5.49	24.2	54.4	0	5.49	24.2	54.4
Tissue/Finding	Number of Animals	10	10	10	10	10	10	10	10
Lung									
Cellularity increased, macrophage, alveolar	Total	0	10	10	10	0	10	10	10
	minimal	—	10	10	10	0	10	10	9
	mild	—	—	—	—	—	—	—	1
Basophilic granulation, intracellular, alveolar macrophage	Total	0	10	10	10	0	10	10	10
	minimal	—	10	10	10	—	10	10	9
	mild	—	—	—	—	—	—	—	1
Tracheobronchial lymph node									
	(Number examined)	*9*	*8*	*9*	*9*	*10*	*10*	*9*	*8*
Cellularity increased, macrophage, sinus	Total	0	5	7	9	0	4	9	8
	minimal	—	5	7	9	—	4	9	8
Basophilic granulation, intracellular, macrophage	Total	0	5	7	9	0	4	9	8
	minimal	—	5	7	9	—	4	9	8
Mandibular lymph node									
	(Number examined)	*9*	*10*	*10*	*10*	*9*	*10*	*10*	*10*
Cellularity increased, macrophage, sinus	Total	0	0	0	3	0	0	0	2
	minimal	—	—	—	3	—	—	—	2
Basophilic granulation, intracellular, macrophage	Total	0	0	0	3	0	0	0	2
	minimal	—	—	—	3	—	—	—	2
Kidney									
Basophilic granulation, tubule	Total	0	0	0	8	0	0	1	8
	minimal	—	—	—	8	—	—	1	8
Liver									
Basophilic granulation, Kupffer cell	Total	0	0	0	0	0	0	0	5

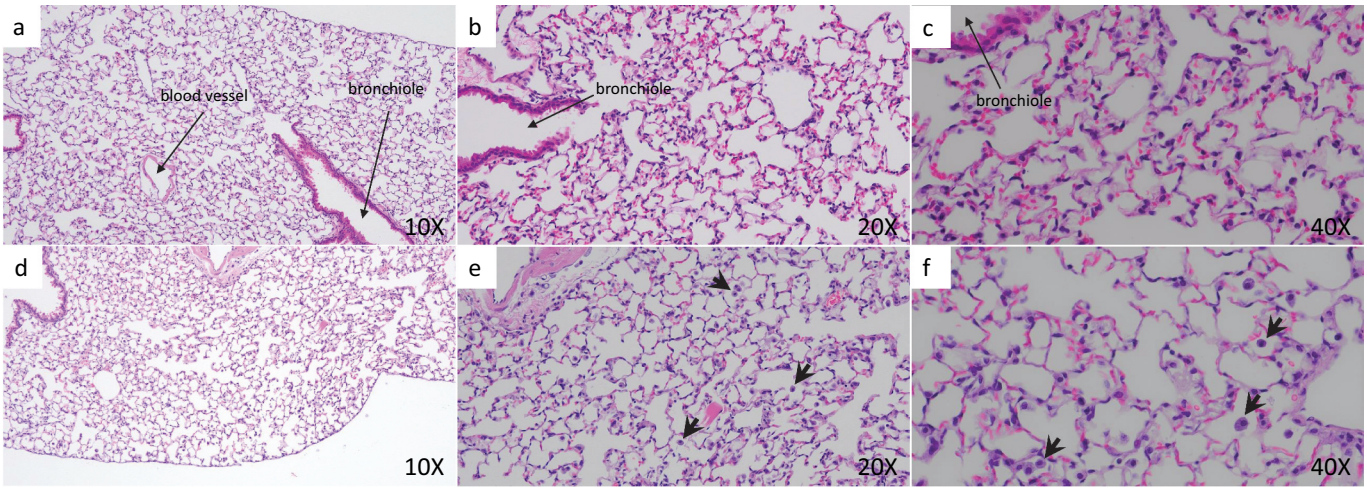

Figure 2. Representative H&E lung sections from main phase control mice (A-C) and SPL84-treated mice (54.4 mg/kg/week, D-F). Alveolar macrophages with basophilic granules (thick arrows).

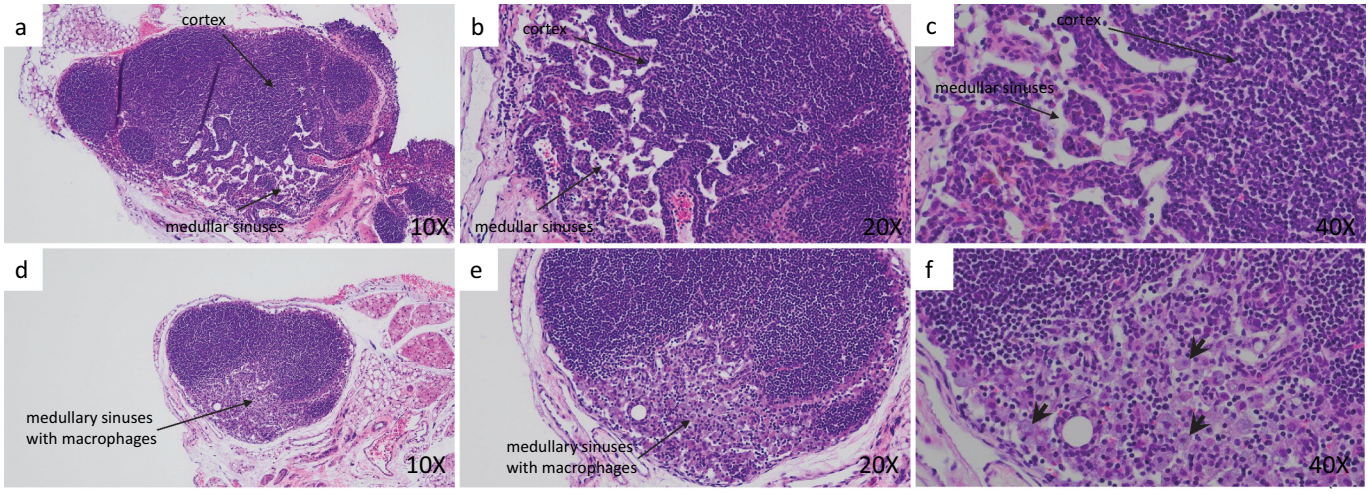

Figure 3. Representative H&E tracheabronchial lymph node sections from main phase control mice (A-C) and SPL84-treated mice (54.4 mg/kg/week, D-F). Alveolar macrophages with basophilic granules (thick arrows).

In monkeys, inhalation administration of SPL84 was well tolerated as there was no mortality, and no SPL84-related clinical signs or changes in body weight, ophthalmology, clinical pathology parameters (hematology, coagulation, clinical chemistry, and urinalysis), alternative complement pathway activation, organ weights, and macroscopic observations. Microscopic findings related to the administration of SPL84 were noted in the lungs and tracheobronchial lymph node (Table 4a,b). Minimal to mild accumulation of alveolar macrophages with basophilic vacuolated cytoplasm in the lungs and mild to moderate accumulation of macrophages with basophilic vacuolated cytoplasm in the medulla of the tracheobronchial lymph node were observed in all animals treated with SPL84 with some signs of a dose relationship. There were no microscopic findings in any other organs. Following the 12-week recovery period, dose-related minimal to mild accumulation of alveolar macrophages with basophilic vacuolated cytoplasm in the lungs and mild to marked accumulation of macrophages with basophilic vacuolated cytoplasm in the medulla of the tracheobronchial lymph node were observed (Supp Table S8). The severity of these findings was lower when compared with the findings of the main animals, indicative of partial recovery. These findings were not considered adverse. Given the non-adverse nature of the findings and ongoing recovery, the NOAEL in monkeys was the highest level of 20.8 mg/kg/week.

3.4.3. Toxicokinetics

Toxicokinetic evaluation was performed in plasma on two occasions, following the first dose on Day 1 and after the last dose on Day 57. Plasma concentrations over time are shown in Figure 4a,b, and the toxicokinetic parameters are shown in Table 5. Over the dose range, exposure to SPL84 (based on Cmax and AUC values) increased dose-dependently, tended to be dose-proportional, and was generally low. Accumulation ratios (based on AUC0-Tlast) suggested that SPL84 did not accumulate between Day 1 and Day 57 (Table 5).

Table 4a. Microscopic changes in the lung –monkey toxicity study.

		Male				Female			
	Dose (mg/kg/week)	0	6.0	10.9	20.8	0	6.0	10.9	20.8
Tissue/Finding	Number of Animals	3	3	3	3	3	3	3	3
Lung									
	(Number examined)	*3*	*3*	*3*	*3*	*3*	*3*	*3*	*3*
	No Abnormalities	2	0	0	0	2	0	0	0
Accumulation; macrophage, alveolus	Total	0	3	3	3	0	3	3	3
	minimal	0	1	2	0	0	3	2	0
	mild	0	2	1	3	0	0	1	3
Fibrosis; pleura	Total	0	0	0	0	0	0	0	1
	mild	0	0	0	0	0	0	0	1
Granuloma	Total	1	0	0	0	0	0	0	0
	present	1	0	0	0	0	0	0	0
Infiltrate; mixed cell	Total	0	1	0	0	0	0	0	0
	minimal	0	1	0	0	0	0	0	0
Infiltrate; mononuclear cell, perivascular	Total	0	0	0	2	1	0	0	1
	minimal	0	0	0	2	1	0	0	1
Infiltrate; neutrophil, alveolus	Total	0	0	0	0	0	1	0	0
	minimal	0	0	0	0	0	1	0	0
Infiltrate; neutrophil, alveolus; perivascular	Total	0	0	0	0	0	0	0	1
	minimal	0	0	0	0	0	0	0	1

Table 4b. Microscopic changes in the tracheo-bronchial, mandibular lymph nodes kidney and liver- monkey toxicity study

		Male				Female			
	Dose (mg/kg/week)	0	6.0	10.9	20.8	0	6.0	10.9	20.8
Tissue/Finding	Number of Animals	3	3	3	3	3	3	3	3
Tracheo-bronchial lymph node									
	(Number examined)	*3*	*3*	*3*	*3*	*3*	*3*	*3*	*3*
	No Abnormalities	3	0	0	0	3	0	0	0
Accumulation; macrophage, alveolus	**Total**	0	3	3	3	0	3	3	3
	mild	0	1	2	0	0	3	1	0
	moderate	0	2	1	3	0	0	2	3
Cellularity, increased; lymphocyte	**Total**	0	0	1	0	0	0	0	0
	mild	0	0	1	0	0	0	0	0
Mandibular lymph node									
	(Number examined)	*3*	*0*	*0*	*3*	*3*	*0*	*0*	*3*
	No Abnormalities	3	-	-	1	3	-	-	3
Infiltrate; inflammatory cell, medulla	**Total**	0	-	-	2	0	-	-	0
	minimal	0	-	-	1	0	-	-	0
	mild	0	-	-	1	0	-	-	0
Kidney									
	(Number examined)	*3*	*0*	*0*	*3*	*3*	*0*	*0*	*3*
	No Abnormalities	1	-	-	3	2	-	-	2
Infiltrate; mononuclear cell, cortex	**Total**	2	-	-	0	1	-	-	1
	minimal	2	-	-	0	1	-	-	1
Liver									
	(Number examined)	*3*	*0*	*0*	*3*	*3*	*0*	*0*	*3*
	No Abnormalities	3	-	-	3	-	-	-	3

3.4.4. Tissue distribution

The tissue levels of SPL84 were measured in the lungs, liver, and kidney samples collected from the mouse toxicity study on Days 1 and 57 at 1 hr and 24 hrs post-end of exposure, as well as following the recovery period (high dose groups only). SPL84 levels measured in lungs, liver, and kidney at each timepoint are presented in Figure 5. As expected, mean levels of SPL84 measured in the lung on Day 57 were greater compared to Day 1, increased with dose, and were greater 1-hour post-end of exposure compared to 24 hours post-end of exposure in the mid and high dose groups (but similar in the low dose group). Similarly, in liver and kidney samples, mean levels of SPL84 measured on Day 57 were greater compared to Day 1, increased with dose, and were greater 24 hours post-end of exposure compared to levels measured 1 hour post-end of exposure. The mean levels of SPL84 in liver and kidney were substantially lower than lung levels for all dose levels. Following the 12-week recovery period, SPL84 continued to be measurable in lung, liver and kidney samples but at much lower levels compared to the end of the treatment period on Day 57. The levels of SPL84 in the lung at recovery were similar between the mid and high dose group, suggesting a plateau may have been reached.

4. Discussion

ASO therapeutics have demonstrated potential to treat many genetic diseases that were once considered untreatable, or for

Table 5. Mean toxicokinetic parameters of SPL84 in mouse and monkey on days 1 and 57 of 8-week toxicity studies.

Species	Achieved Dose (mg/kg/week)	Day	Cmax (µg/ml) ±SEM	Tmax (hrs) ±SEM	AUC0-Tlast (µg/ml*hrs) ±SEM	T1/2 (hrs) ±SEM
Mouse	5.49	1	0.146	0.5	0.598	3.725
	24.2		0.816	0.75	3.26	4.015
	54.4		2.16	0.75	7.355	4.865
	5.49	57	0.2125	0.5	0.7955	4.825
	24.2		0.62	1	3.75	5.47
	54.4		1.77	0.5	6.85	5.265
Monkey	5.9	1	0.284 ± 0.04	3.67 ± 0.95	3.628 ± 0.44	8.67 ± 0.59
	10.9		0.75 ± 0.102	1.7 ± 0.2	7.523 ± 0.76	7.98 ± 0.31
	20.8		1.843 ± 0.31	1.85 ± 0.15	15.114 ± 2.02	8.18 ± 0.59
	5.9	57	0.252 ± 0.039	2.67 ± 0.42	3.437 ± 0.45	9.9 ± 0.49
	10.9		0.616 ± 0.06	2.2 ± 0.2	7.504 ± 0.68	15.2 ± 0.52*
	20.8		2.05 ± 0.46	1.85 ± 0.1	21.067 ± 3.27	17.2 ± 0.45*

*T1/2 was calculated including the 96-hour timepoint for the recovery animals (n = 2/sex/group).

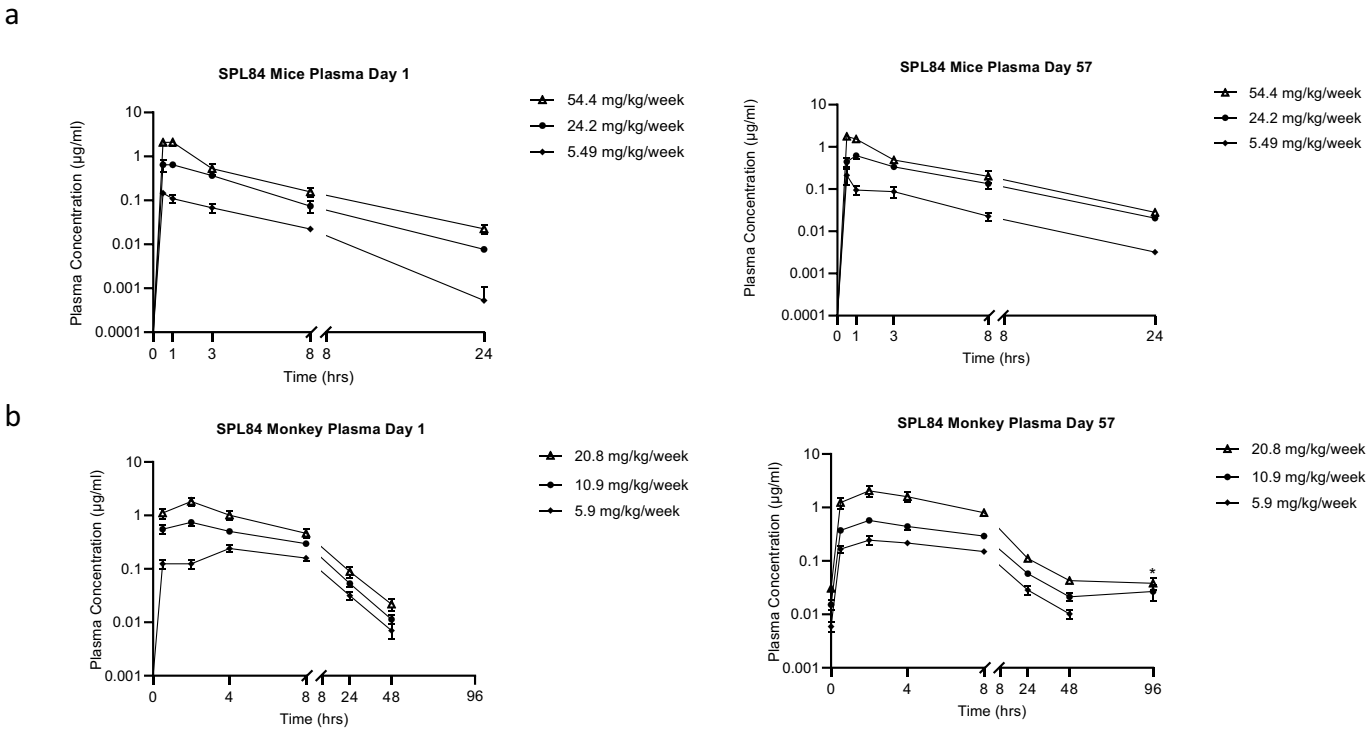

Figure 4. Plasma concentration vs time of SPL84 in mice and monkeys. a. Mean (±SEM) plasma concentration vs time profiles of SPL84 following weekly inhalation administration of SPL84 to mice on Day 1 (left) and Day 57 (right) at the following achieved doses: 5.49, 24.2, and 54.4 mg/kg/week (n = 2 animals/sex). b. Mean (±SEM) plasma concentration vs time profiles of SPL84 following weekly inhalation administration of SPL84 to monkeys on Day 1 (left) and Day 57 (right) at the following doses: 5.9,10.9, and 20.8 mg/kg/week (n = 2–5 animals/sex). *These blood samples were collected from the recovery animals of the groups of 10.9 and 20.8 mg/kg/week only on Day 57.

which there were limited therapeutic options. The clinical development of new ASOs for the treatment of a range of human diseases is progressing at a rapid pace, with six new products approved in the past 8 years [36]. These advancements are due in part to the improved metabolic stability of ASOs as well as increased binding affinities. However, challenges remain in ASO drug development, mainly surrounding achieving delivery to target tissues while minimizing local and systemic toxicity, circumventing endosomal trapping, and understanding the preclinical pharmacokinetic/pharmacodynamic relationship and its translation for human dose predictions.

In this study, we describe the nonclinical safety and toxicology studies performed with SPL84, an inhaled ASO drug for the treatment of CF patients (carrying the 3849 CFTR mutation). These studies were all submitted to the regulatory authorities for approval of a first-in-human clinical study with SPL84, which is currently ongoing. Toxicology studies demonstrated no SPL84-related clinical signs, nor any effect on body weight, food consumption, clinical chemistry, hematology, or organ weights, and all microscopic changes were considered non-adverse. Moreover, SPL84 was shown not to be genotoxic, nor to have mutagenic potential, and had no effect in a complete battery of safety pharmacology studies (data not shown). In addition, no effect on WT CFTR RNA was observed when tested in epithelial bronchial cells of healthy individuals, and no off-target effect on other genes was observed. SPL84 is not expected to be a substrate of CYP450 as

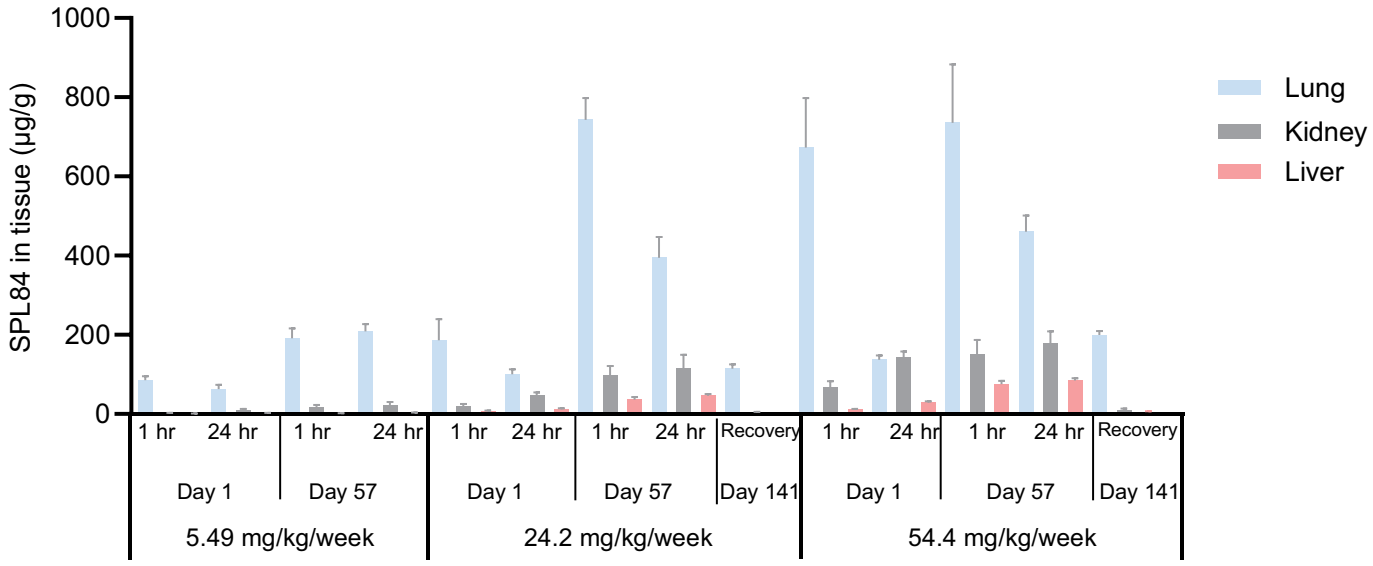

Figure 5. Tissue levels of SPL84 in selected mice tissues. Mean (±SEM) tissue concentrations of SPL84 in the lungs, liver, and kidney following weekly inhalation administration to mice at the following doses: 5.49,24.2, and 54.4 mg/kg/week ($n = 4–6$ animals).

ASOs are not CYP substrates and no drug – drug interactions have been reported for any clinical ASO drug [37]. The NOAEL in the 8-week toxicity studies was determined to be 54.4 and 20.8 mg/kg/week for mice and monkeys, respectively, which provided sufficient safety margins of ~ 40-times the starting clinical dose.

SPL84 is chemically modified with 2′-O-MOE and a phosphorothioate backbone. This second-generation ASO modification has a decreased rate of metabolism compared to the first-generation compounds, resulting in increased tissue residence times. Additionally, a higher percentage of intact oligonucleotide versus metabolites was observed in tissues with 2′-O-MOE phosphorothioate ASOs [38]. As a result of the slower clearance from the tissues and the increased percentage of active compound in the tissues combined with SPL84 potency and full restoration of CFTR as presented before [19], lower doses and/or less frequent dosing may be efficacious with 2′-O-MOE phosphorothioate ASOs [39]. On the other hand, the presumed beneficial therapeutic effects of prolonged tissue residence time and consequently tissue accumulation can increase the potential for tissue toxicity. However, such effects have not been observed with 2′-O-MOE phosphorothioate ASOs. Their safety and pharmacokinetic profiles have been demonstrated in this study and in previous studies performed with 2′-O-MOE phosphorothioate ASOs [40].

An advantage of SPL84 as an inhaled drug is the ability to deliver the ASO therapy directly to the intended target organ, the lung. Pulmonary delivery via inhalation ensures that the ASO is efficiently distributed in the lungs while minimizing systemic exposure and reducing the risk for adverse effects on internal organs as well as known blood-level-related toxicities [41]. Indeed, as expected with inhalation delivery and direct exposure to the lung, the highest concentrations of SPL84 in mice and monkeys following 9 weekly administrations were found in the lung, with substantially lower levels in the liver and kidney. Thus, these results support the specificity of the pulmonary route of administration of SPL84, limiting the systemic exposure and distribution to other tissues. SPL84 was measured in the liver and kidney, which are the major tissues of uptake and clearance of ASOs [42]. Furthermore, the plasma concentrations for the highest doses administered at Cmax were ~2 µg/ml for both mice and monkeys. This is significantly lower than the reported ASO levels measured in animals given intravenous doses of ASOs and levels known to trigger effects to the alternative complement pathway [23,43].

The histological observations described in these studies (Tables 3 and 4a) are most likely related to the normal physiological role of macrophages in the uptake and clearance of ASOs, regardless of the method of administration [24,44,45]. The increased numbers of macrophages in the alveoli are commonly observed with inhalation administration of phosphorothioate oligonucleotides like SPL84 and very likely reflect a normal non-adverse clearance mechanism. The basophilic granulation observed within the alveolar macrophages, kidney tubules, and liver Kupffer cells is a well-recognized benign histomorphologic change that simply reflects the uptake of the oligonucleotide into those cells and sequestering within the endosomal compartment [39,46]. The presence of increased number of macrophages with basophilic inclusions in the proximal mandibular and tracheobronchial lymph node is suggestive of trafficking of these cells from the airway to the local lymph nodes as part of the airway clearance process. Furthermore, similar changes related to the uptake and clearance of ASOs have been described previously with inhaled phosphorothioate oligonucleotides in mice and monkeys [24,27,28]. Lung inflammation has been also demonstrated for approved inhaled drugs for CF and other pulmonary diseases, confirming that this effect is related to delivery regardless of the drug type and, generally, has no toxicological relevance that predicts unacceptable risk in humans. For example, the finding of increased alveolar macrophages was documented in inhalation toxicology studies supporting the registration of Advair [47], Alvesco [48], Cayston [49], and TOBI [50].

Taken together, the pharmacological effect of CFTR functional rescue by SPL84 demonstrated in patient-derived respiratory cells [19] with the proven efficient delivery to lung epithelial

cells [51] (unpublished work), along with the favorable safety profile, supports the development of SPL84 as a promising drug for the treatment of CF patients carrying the 3849 mutation.

5. Conclusion

ASO therapeutics have considerable potential to contribute significantly to the future of medicine, as evidenced by the clinical benefit observed in SMA, familial hypercholesterolemia, and DMD indications [52–54]. Inhalation delivery of SPL84 provides the opportunity for specific gene modulation in the lungs of CF patients. A full battery of safety pharmacology and toxicological studies were completed with SPL84, which demonstrated a favorable profile with no adverse findings or safety issues. The promising safety profile as demonstrated in the described studies is driven by the durability and potency of SPL84 which allow low frequency of administration (weekly or less) and low doses and is being tested in the clinical setting. These results are promising and encouraging for future development of a new generation of ASO-mediated therapies capable of treating various other severe pulmonary diseases.

Funding

This paper was funded by SpliSense LTD.

Declaration of interest

O Barchard-Avitzur, L Friedman, E Ozeri-Galai, A Choen, S Dahan, T Mordechai, and G Hart have been under the employment of SpliSense LTD. The authors have no other relevant affiliations or financial involvement with any organization or entity with a financial interest in or financial conflict with the subject matter or materials discussed in the manuscript. This includes employment, consultancies, honoraria, stock ownership or options, expert testimony, grants or patents received or pending, or royalties.

Reviewer disclosures

Peer reviewers on this manuscript have no relevant financial or other relationships to disclose.

Authorship Contribution Statement:

L Friedman and O Barchard-Avitzur contributed equally to the manuscript. O Barchard-Avitzur was responsible for manuscript organization and writing and carried out the off-target analysis. L Friedman and G Hart: carried out the overall project design, animal studies and tissue analyses, and review and editing. E Ozeri-Galai provided scientific input on specificity and off-target analyses. N Ferrari supervised all the toxicological studies and review and editing. A Choen supported all the CMC aspects for this project. S.D and T Mordechai carried out the specificity and in vitro off target analysis.

Acknowledgments

The authors are grateful to Dr. D Kornbrust (Preclinsight) and R Wolff (RK Wolff Safety Consulting Inc) for toxicity input and discussion along the project. Monoceros Biosystems LLC for the in silico off-target analysis. ImmunXperts (Belgium) for executing PBMC cytokine release assay (CRA). ITR Laboratories and Axolabs GmbH for executing all the toxicological studies.

Ethics Statement

The study plans and relevant amendments were reviewed and approved by the Animal Care Committee (ACC) of ITR. ACC acceptance was maintained on file at ITR. All animals used in the study were cared for in accordance with the principles outlined in the current 'Guide to the Care and Use of Experimental Animals' as published by the Canadian Council on Animal Care and the 'Guide for the Care and Use of Laboratory Animals,' a NIH publication.

References

1. Beaudet AL, Meng L. Gene-targeting pharmaceuticals for single-gene disorders. Hum Mol Genet. 2016;25:R18–26. doi: 10.1093/hmg/ddv476
2. McClorey G, Wood MJ. An overview of the clinical application of antisense oligonucleotides for RNA-targeting therapies. Curr Opin Pharmacol. 2015;24:52–58. doi: 10.1016/j.coph.2015.07.005
3. Lee RG, Crosby J, Baker BF, et al. Antisense technology: an emerging platform for cardiovascular disease therapeutics. J Cardiovasc Transl Res. 2013;6:969–980. doi: 10.1007/s12265-013-9495-7
4. Rigo F, Hua Y, Krainer AR, et al. Antisense-based therapy for the treatment of spinal muscular atrophy. J Cell Bio. 2012;199:21–25. doi: 10.1083/jcb.201207087
5. Bennett CF, Swayze EE. RNA targeting therapeutics: molecular mechanisms of Antisense oligonucleotides as a therapeutic platform. Annu Rev Pharmacol Toxicol. 2010;50:259–293. doi: 10.1146/annurev.pharmtox.010909.105654
6. Crooke ST, editor. Antisense drug technology. CRC Press; 2007. doi: 10.1201/9780849387951
7. Geary RS, Watanabe TA, Truong L, et al. Pharmacokinetic properties of 2′-O-(2-methoxyethyl)-modified oligonucleotide analogs in rats. J Pharmacol Exp Ther. 2001;296(3):890–897.
8. Lima WF, Vickers TA, Nichols J, et al. Defining the factors that contribute to on-target specificity of antisense oligonucleotides. PLoS One. 2014;9(7):e101752. doi: 10.1371/journal.pone.0101752
9. Crooke ST, Baker BF, Crooke RM, et al. Antisense technology: an overview and prospectus. Nat Rev Drug Discov. 2021;20(6):427–453. doi: 10.1038/s41573-021-00162-z
10. Fey R, Zanardi T, Kramer-Stickland K, et al. Toxicologic properties of 2′-O-Methoxyethyl Chimeric Antisense inhibitors in animals and man. Antisense Drug Technol. 2007;327–363. CRC Press. doi: 10.1201/9780849387951.ch12
11. Yu R, Geary R, Siwkowski A, et al. Pharmacokinetic/Pharmacodynamic properties of Phosphorothioate 2′-O-(2-methoxyethyl)-Modified Antisense oligonucleotides in animals and man. Antisense Drug Technol. 2007;305–326. CRC Press. doi: 10.1201/9780849387951.ch11
12. Geary RS. Antisense oligonucleotide pharmacokinetics and metabolism. Expert Opin Drug Metab Toxicol. 2009;5:381–391. doi: 10.1517/17425250902877680
13. Yu RZ, Grundy JS, Geary RS. Clinical pharmacokinetics of second generation antisense oligonucleotides. Expert Opin Drug Metab Toxicol. 2013;9:169–182. doi: 10.1517/17425255.2013.737320
14. Egli M, Manoharan M. Chemistry, structure and function of approved oligonucleotide therapeutics. Nucleic Acids Res. 2023;51:2529–2573. doi: 10.1093/nar/gkad067
15. Kim J, Hu C, Moufawad El Achkar C, et al. Patient-customized oligonucleotide therapy for a Rare genetic disease. N Engl J Med. 2019;381(17):1644–1652. doi: 10.1056/nejmoa1813279
16. Highsmith WE, Burch LH, Zhou Z, et al. A novel mutation in the cystic fibrosis gene in patients with pulmonary disease but normal sweat chloride concentrations. N Engl J Med. 2010;331(15):974–980. doi: 10.1056/NEJM199410133311503
17. Linde L, Boelz S, Nissim-Rafinia M, et al. Nonsense-mediated mRNA decay affects nonsense transcript levels and governs response of cystic fibrosis patients to gentamicin. J Clin Invest. 2007;117:683–692. doi: 10.1172/JCI28523
18. Nissim-Rafinia M, Aviram M, Randell SH, et al. Restoration of the cystic fibrosis transmembrane conductance regulator function by

splicing modulation. EMBO Rep. 2004;5(11):1071–1077. doi: 10.1038/sj.embor.7400273
19. Oren YS, Irony-Tur Sinai M, Golec A, et al. Antisense oligonucleotide-based drug development for cystic fibrosis patients carrying the 3849+10 kb C-to-T splicing mutation. J Cyst Fibros. 2021;20:865–875. doi: 10.1016/j.jcf.2021.06.003
20. Levin AA. A review of issues in the pharmacokinetics and toxicology of phosphorothioate antisense oligonucleotides. Biochim Biophys Acta - Gene Struct Expr. 1999;1489(1):69–84. doi: 10.1016/S0167-4781(99)00140-2
21. Danahay H, Giddings J, Christian RA, et al. Distribution of a 20-mer phosphorothioate oligonucleotide, CGP69846A (ISIS 5132), into airway leukocytes and epithelial cells following intratracheal delivery to brown-norway rats. Pharm Res. 1999;16:1542–1549. doi: 10.1023/a:1015048419558
22. Geary RS, Yu RZ, Watanabe T, et al. Pharmacokinetics of a tumor necrosis factor -α phosporothioate 2′- O -(2-methoxyethyl) modified antisense oligonucleotide: comparison across species. Drug Metab Dispos. 2003;31(11):1419–1428. doi: 10.1124/dmd.31.11.1419
23. Geary RS, Leeds JM, Fitchett J, et al. Pharmacokinetics and metabolism in mice of a phosphorothioate oligonucleotide antisense inhibitor of C-raf-1 kinase expression. Drug Metab Dispos. 1997;25(11):1272–1281.
24. Templin MV, Levin AA, Graham MJ, et al. Pharmacokinetic and toxicity profile of a phosphorothioate oligonucleotide following inhalation delivery to lung in mice. Antisense Nucleic Acid Drug Dev. 2000;10(5):359–368. doi: 10.1089/oli.1.2000.10.359
25. Chi KN, Eisenhauer E, Fazli L, et al. A phase I pharmacokinetic and pharmacodynamic study of OGX-011, a 2′-methoxyethyl antisense oligonucleotide to clusterin, in patients with localized prostate cancer. J Natl Cancer Inst. 2005;97:1287–1296. doi: 10.1093/jnci/dji252
26. Tolcher AW, Chi K, Kuhn J, et al. A phase II, pharmacokinetic, and biological correlative study of oblimersen sodium and docetaxel in patients with hormone-refractory prostate cancer. Clin Cancer Res. 2005;11:3854–3861. doi: 10.1158/1078-0432.CCR-04-2145
27. Fey RA, Templin MV, McDonald JD, et al. Local and systemic tolerability of a 2′O-methoxyethyl antisense oligonucleotide targeting interleukin-4 receptor-α delivery by inhalation in mouse and monkey. Inhal Toxicol. 2014;26(8):452–463. doi: 10.3109/08958378.2014.907587
28. Guimond A, Viau E, Aubé P, et al. Advantageous toxicity profile of inhaled antisense oligonucleotides following chronic dosing in non-human primates. Pulm Pharmacol Ther. 2008;21:845–854. doi: 10.1016/j.pupt.2008.08.001
29. Ali S, Leonard SA, Kukoly CA, et al. Absorption, distribution, metabolism, and excretion of a respirable antisense oligonucleotide for asthma. Am J Respir Crit Care Med. 2001;163(4):989–993. doi: 10.1164/ajrccm.163.4.9907078
30. Pranke IM, Hatton A, Simonin J, et al. Correction of CFTR function in nasal epithelial cells from cystic fibrosis patients predicts improvement of respiratory function by CFTR modulators. Sci Rep. 2017;7(1):1–11. doi: 10.1038/s41598-017-07504-1
31. Lindow M, Vornlocher H-P, Riley D, et al. Assessing unintended hybridization-induced biological effects of oligonucleotides. Nat Biotechnol. 2012;30(10):920–923. doi: 10.1038/nbt.2376
32. Alexander DJ, Collins CJ, Coombs DW, et al. Association of inhalation Toxicologists (AIT) working party recommendation for standard delivered dose calculation and expression in non-clinical aerosol inhalation toxicology studies with pharmaceuticals. Inhal Toxicol. 2008;20:1179–1189. doi: 10.1080/08958370802207318
33. Krieg AM. The CpG motif. BioDrugs. 1998;10(5):341–346. doi: 10.2165/00063030-199810050-00001
34. Zhao Q, Temsamani J, Iadarola PL, et al. Effect of different chemically modified oligodeoxynucleotides on immune stimulation. Biochem Pharmacol. 1996;51:173–182. doi: 10.1016/0006-2952(95)02177-9
35. Agrawal S, Kandimalla ER. Antisense and siRNA as agonists of Toll-like receptors. Nat Biotechnol. 2004;22(12):1533–1537. doi: 10.1038/nbt1042
36. Kulkarni JA, Witzigmann D, Thomson SB, et al. The current landscape of nucleic acid therapeutics. Nat Nanotech. 2021;16:630–643. doi: 10.1038/s41565-021-00898-0
37. FDA. Clinical pharmacology considerations for the development of oligonucleotide therapeutics guidance for industry clinical pharmacology considerations for the development of oligonucleotide therapeutics guidance for industry. J Oral Biol Craniofac Res. 2022;12(4):410–412. doi: 10.1016/j.jobcr.2022.04.010
38. Henry SP, Geary RS, Yu R, et al. Drug properties of second-generation antisense oligonucleotides: how do they measure up to their predecessors? Curr Opin Invest Drugs. 2001;2(10):1444–1449.
39. Levin AA, Henry SP, Monteith D. Toxicity of Antisense oligonucleotides. In: Crooke ST. Antisense Drug Technol Princ Strateg Appl. Basel/New York: Marcel Deker; 2001. p. 201–267.
40. Farman CA, Kornbrust DJ. Oligodeoxynucleotide studies in primates: antisense and immune stimulatory indications. Toxicol Pathol. 2003;31(1):119–122. doi: 10.1080/01926230390174995
41. Geary RS, Norris D, Yu R, et al. Pharmacokinetics, biodistribution and cell uptake of antisense oligonucleotides. Adv Drug Deliv Rev. 2015;87:46–51. doi: 10.1016/j.addr.2015.01.008
42. Geary RS, Leeds JM, Henry SP, et al. Antisense oligonucleotide inhibitors for the treatment of cancer: 1. Pharmacokinetic properties of phosphorothioate oligodeoxynucleotides. Anticancer Drug Des. 1997;12(5):383–393.
43. Yu RZ, Geary RS, Monteith DK, et al. Tissue disposition of 2′-O-(2-methoxy) ethyl modified Antisense oligonucleotides in monkeys. J Pharm Sci. 2004;93:48–59. doi: 10.1002/jps.10473
44. Burger GT, Renne RA, Sagartz JW, et al. Histologic changes in the respiratory tract induced by inhalation of xenobiotics: physiologic adaptation or toxicity? Toxicol Appl Pharmacol. 1989;101:521–542. doi: 10.1016/0041-008X(89)90200-7
45. Nikula KJ, McCartney JE, McGovern T, et al. STP position paper. Toxicol Pathol. 2014;42(3):472–486. doi: 10.1177/0192623313507003
46. Frazier KS. Antisense oligonucleotide therapies: the promise and the challenges from a toxicologic Pathologist's perspective 2015. doi: 10.1177/0192623314551840
47. Toxicology review of Advair for NDA, 2006.
48. Pharmacology and toxicology of Alvesco review for NDA. 1997.
49. Cayston EPAR product information. 2016. 116–130. doi: 10.2307/j.ctv24q4zdn.23
50. Pharmacology and toxicology of TOBI review for NDA. 1997.
51. Ozeri-Galai E. Delivery characterization of SPL84 inhaled Antisense oligonucleotide drug for 3849 + 10 kb C- > T cystic fibrosis patients. Nucleic Acid Ther. 2023;1–20. doi: 10.1089/nat.2023.0015
52. Ottesen EW, News Release. FDA approves first drug for spinal muscular atrophy. Translational Neuroscience. 2017;8(1):1–6. doi: 10.1515/tnsci-2017-0001
53. Nusinersen C. Biogen and ionis pharmaceuticals report nusinersen meets primary endpoint at interim analysis of phase 3 ENDEAR study in infantile-onset spinal muscular atrophy. Biog Press Release. Aug 1 2016accessed Jul 5, 2021;8–11. https://investors.biogen.com/news-releases/news-release-details/biogen-and-ionis-pharmaceuticals-report-nusinersen-meets-primary
54. FDA grants accelerated approval to first drug for duchenne muscular dystrophy. Case Med Res. 2016. doi: 10.31525/cmr-29dc5f3